Texture of Crystalline Solids
1978, Vol. 3, pp. 53-72

EFFECT OF CARBIDE SIZE, COLD REDUCTION AND HEATING RATE IN ANNEALING ON DEEP-DRAWABILITY OF LOW-CARBON, CAPPED COLD-ROLLED STEEL SHEET

KAZUO MATSUDO, TAKAYOSHI SHIMOMURA and OSAMU NOZOE

Fukuyama Research Laboratories, Technical Research Center, Nippon Kokan K.K., Hiroshima, 721 Japan

(Received October 27, 1977)

Abstract: The effects of carbide size prior to cold rolling, cold reduction and heating rate in annealing on $\bar{r}$-value, and texture of cold-rolled steel sheets were investigated. The main results obtained were as follows: (1) When the carbide size prior to cold rolling is large, $\bar{r}$-value can be improved with a faster heating rate in annealing. (2) Moreover, the cold reduction of peak $\bar{r}$-value shifts to the higher cold reduction side, and $\bar{r}$-value tends to increase with cold reduction up to 90%. These phenomena are thought to be based on the delay in dissolution of carbide at the initial state of recrystallization, the change in recrystallization temperature and the preferred nucleation.

1. INTRODUCTION

Various studies on the deep-drawability of cold-rolled steel sheet have been conducted by many investigators since Lankford[1] advocated the plastic anisotropy, i.e., r-value, as a new criterion for evaluating the deep-drawability of cold-rolled steel sheet. The effect of various factors in the manufacture of cold-rolled steel sheets on deep drawability has now been clarified considerably.

As to the effect of cold-reduction which is one of the manufacturing factors on the deep drawability, many reports[3-6] by Whiteley[2] and other investigators have been presented. It is well known that $\bar{r}$-value varies with cold reduction and that there is a certain cold reduction at which the $\bar{r}$-value shows a maximum. According to most of the reports, the cold reduction of peak $\bar{r}$-value ranges from 60 to 70%. Whiteley et al. have explained this phenomenon based on the changes in {222} and {200} texture. It is well known that this cold

reduction of peak $\bar{r}$-value is influenced by the various processing factors, such as chemical compositions and cold-rolling lubricants, etc.[3-5,7-9] The authors have experienced in many instances that the cold reduction of the peak $\bar{r}$-value is near 80%.

Fukuda[3] and the authors[5] have studied the effect of carbon content on r-value and reported that the peak $\bar{r}$-value moves to the higher cold reduction side as carbon content decreases. Also, Held[8] and the authors have reported that the texture in the normal direction changes considerably due to the conditions of lubricants used in cold-rolling, thereby exerting influence on the $\bar{r}$-value.

Urged by the necessity of rationalization and labor saving in recent years, the authors have succeeded in the development of a new continuous annealing system of drawing quality steel sheet. It is one of the key points of this system that a hot strip is coiled at high temperatures. Coarse cementite developed by high-temperature coiling exerts influence on the subsequent conditions of cold rolling and annealing: when a hot strip with coarse cementite is cold-rolled and then annealed rapidly as in continuous annealing process, a recrystallized texture having stronger {222} intensities and weaker {200} intensities is developed, and the $\bar{r}$-value becomes higher. Furthermore, it has been recognized that the cold reduction of the peak $\bar{r}$-value of steels having coarse cementite moves to the higher cold reduction side in rapid annealing.

In view of these facts, the authors have studied the effect of carbide size prior to cold rolling, cold reduction, and heating rate in annealing on $\bar{r}$-value and texture.

2. EXPERIMENTAL PROCEDURES

2-1 *Materials*

The materials used in the present investigation were 3.2 mm thick hot-rolled sheets of low carbon capped steel. Chemical compositions and hot rolling conditions are shown in Table I.

TABLE I. Chemical compositions and hot rolling conditions

Hot-rolled sheet thickness (mm)	Hot rolling conditions (°C)		Chemical compositions (wt. %)					
	Finishing temp.	Coiling temp.	C	Mn	P	S	N	O
3.2	860	600	0.055	0.38	0.010	0.024	0.0019	0.037

2-2 *Experimental procedures*

The experimental procedures are shown in Figure 1. The hot-rolled materials were first normalized at 930°C for 10 minutes in a salt bath to attain uniform ferrite grains,

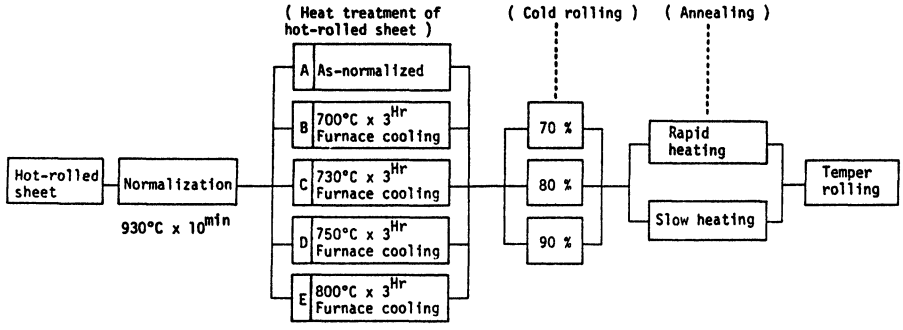

Figure 1. Experimental procedure.

and these materials were heat-treated to change the carbide size in a laboratory furnace in the following manner:

A: As-normalized,
B: 700°C × 3-hr (furnace cool),
C: 730°C × 3-hr (furnace cool),
D: 750°C × 3-hr (furnace cool),
E: 800°C × 3-hr (furnace cool).

After the heat-treatment the materials were cold-rolled on a laboratory mill, 380 mm in diameter and 350 mm in barrel length, using soluble oil. The cold reductions of 70, 80 and 90% were applied.

These cold-rolled materials were annealed in two different cycles: rapid heating assuming continuous annealing and slow heating assuming ordinary box annealing.

Rapid heating was carried out in a salt bath assuming the heating cycle of NKK-CAL System,[10] heating rate (50°C/sec), soaking (700°C), water-quenching and over-aging, and slow heating was carried out in a laboratory furnace (N_2 atmosphere), heating rate (100°C/hr), soaking (700°C) and furnace cooling. These annealing cycles are shown in Figure 2. After annealing, these specimens were temper-rolled to an extension ranging from 1.0 to 1.5%, then tested for r-values.

2-3 *Measuring method*

1) Microstructure: Observations of carbide and ferrite microstructure of heat-treated and annealed materials were conducted.

2) r-value: The r-value was calculated by the following equations using JIS No. 5 test specimens taken from each sample:

$$r = \log (W_0/W)/\log (W \cdot \ell/W_0 \cdot \ell_0) \quad (1)$$

where W_0 and W are the width of parallel portion of the specimen before and after applying elongation strain ($W_0 \approx 25$ mm)

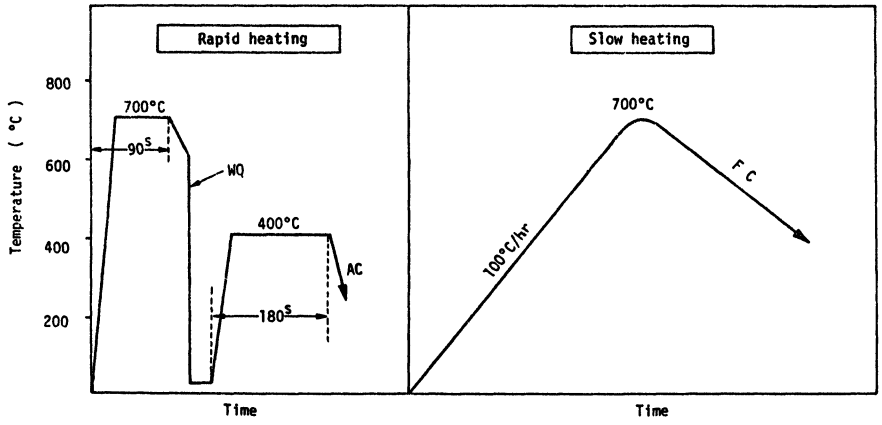

Figure 2. Experimental annealing cycle.

ℓ_0 and ℓ are the gauge length before and after applying elongation strain ($\ell_0 \approx 20$ mm).

All the specimens were measured for r-value in the direction of 0°, 45°, and 90° to the rolling direction, at an elongation strain of about 15%.

After the r-value was measured at each angle, $\bar{r}$ and Δr values were calculated from the following equations:

$$\bar{r} = (r_0 + 2r_{45} + r_{90})/4 \tag{2}$$

$$\Delta r = (r_0 - 2r_{45} + r_{90})/2 \tag{3}$$

where subscripts represent angles to the rolling direction.

3) Texture: The measurement of texture was made by the X-ray integrated reflection intensity, and pole figures were prepared as to the typical test specimens.

The measurement was made at the center of thickness in parallel with the rolling plane. Planes to be measured were machined, paper-finished and chemically polished in an aqueous solution of oxalic acid and hydrogen peroxide.

The integrated reflection intensity was measured at seven plane reflections, {110}, {200}, {112}, {222}, {310}, {123}, and {332} lying parallel with the rolling plane, and the intensity for the random component at each plane (volumetric ratio, P) was calculated by the following equation:[11]

$$P = (Ihk\ell/I^0hk\ell)/(1/n)\cdot\Sigma(Ihk\ell/I^0hk\ell) \tag{4}$$

where $I^0hk\ell$ is the theoretical relative intensity of {hkℓ} plane in randomly oriented grain;
$Ihk\ell$ is the measured intensity of {hkℓ} plane;
n is the number of the planes measured.

The {200} pole figures determined from the midthickness section of typical materials were obtained by both transmission

and reflection methods, and after these figures were adjusted to the same level, they were expressed in the intensity ratio with the mean value of the entire intensity measured being 1 (random intensity).

3. RESULTS

3-1 *Microstructure*

Photograph 1 shows microstructures of ferrite and carbide of the heat-treated materials. Ferrite grains of these heat-treated materials are almost uniform in size. There is little difference in ferrite grain size between these materials. The smallest grain size of heat-treated material A (as normalized) is ASTM No. 8.5, while the largest of heat-treated material E (normalized and heat-treated at 800°C for three hours) is ASTM No. 7.5.

The shape and size of carbide varies with the heat-treatment conditions; that is, the carbides of heat-treated materials A (as-normalized) and B (normalized and heat-treatment at 700°C) are small and are distributed uniformly, and the former is fine pearlite. The carbide size of heat-treated material C (normalized and heat-treated at 730°C) is medium, and those of heat-treated materials D (normalized and heat-treated at 750°C) and E (normalized and heat-treated at 800°C) are large. These large carbides correspond to the carbides formed by high-temperature coiling exceeding A_1-point.

3-2 r-*Value*

Figure 3 shows the change in $\bar{r}$-value by cold reduction and Figure 4, that in Δr-value by cold reduction.

Changes in $\bar{r}$-value due to cold reduction show different tendencies depending on the size of carbide prior to cold-rolling and on the heating rate in annealing. In the case of slow heating as in box-annealing, the $\bar{r}$-value shows the maximum at 80% cold reduction irrespective of the shape and size of the carbide prior to cold-rolling. In the case of rapid heating as in continuous annealing, $\bar{r}$-value varies with the carbide size prior to cold-rolling. As shown in materials D and E, the cold reduction of the peak $\bar{r}$-value moves to the higher cold reduction side as the carbide size prior to cold rolling becomes larger. Under the same cold reduction, slow heating (box-annealing) shows a higher $\bar{r}$-value than in rapid heating (continuous annealing), if the carbide size prior to cold-rolling is small (heat-treated materials A and B). On the contrary, if the carbide size is medium or large (heat-treated materials C, D and E), rapid heating shows a higher $\bar{r}$-value than in slow heating. The materials D and E with large carbides show a higher $\bar{r}$-value than those with small carbides irrespective of the heating rate. This relation is evident from Figure 5, which is rewritten from Figure 3.

The change in Δr-value caused by cold reduction is not clear because the range of cold reductions used in this experiment covered those exceeding the cold reduction of peak Δr-value. It has ever been known that the cold reduction of

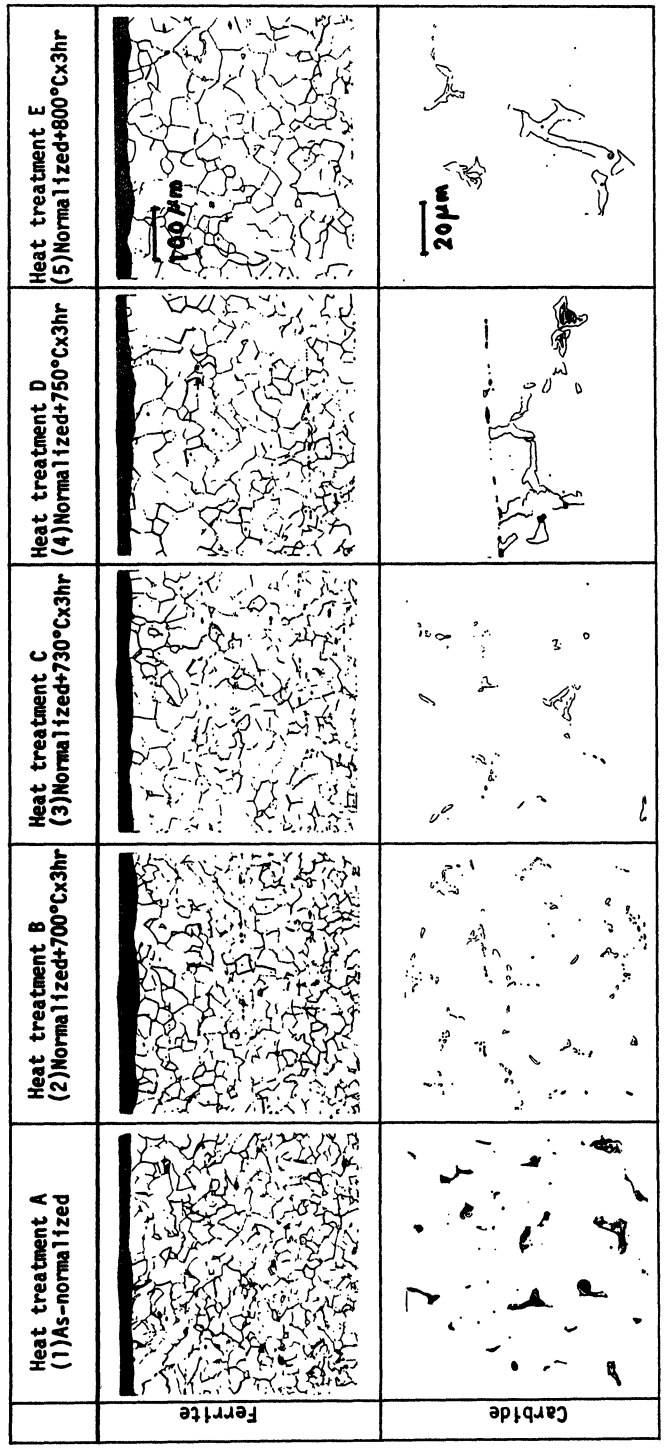

Photograph 1. Ferrite and carbide structures after heat treatment of hot rolled sheet.

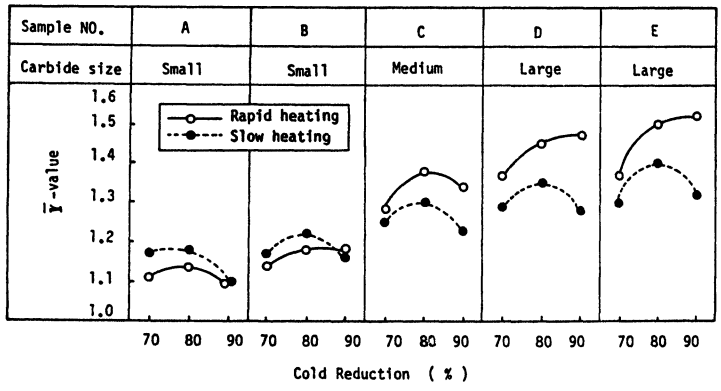

Figure 3. Effect of cold reduction on $\bar{r}$-value.

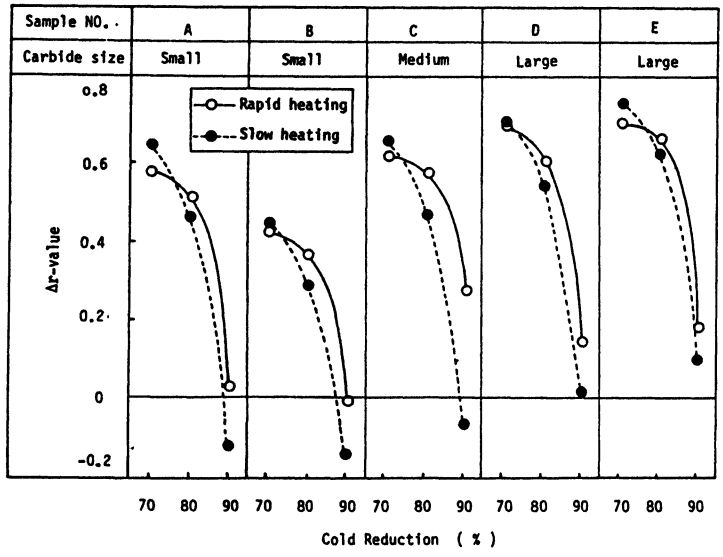

Figure 4. Effect of cold reduction on Δr-value.

peak Δr-value is 60 to 70%.[2,5] Also, judging from the change in Δr-value with cold reduction ranging from 70 to 80%, the cold reduction of the peak Δr-value in rapid heating seems to move somewhat toward the higher cold reduction side than in slow heating. Under the same cold reduction, Δr-value becomes somewhat higher accordingly as the carbide size prior to cold-rolling is larger. For heat-treated material B, the Δr-value at 70 and 80% cold reduction is extremely lower than that of the other heat-treated materials, but the reasons for this are not clear.

In terms of the difference in Δr-value between annealing conditions, the value is approximately the same or a little higher in slow heating at 70% cold reduction, while the Δr-value tends to become higher in rapid heating at a cold

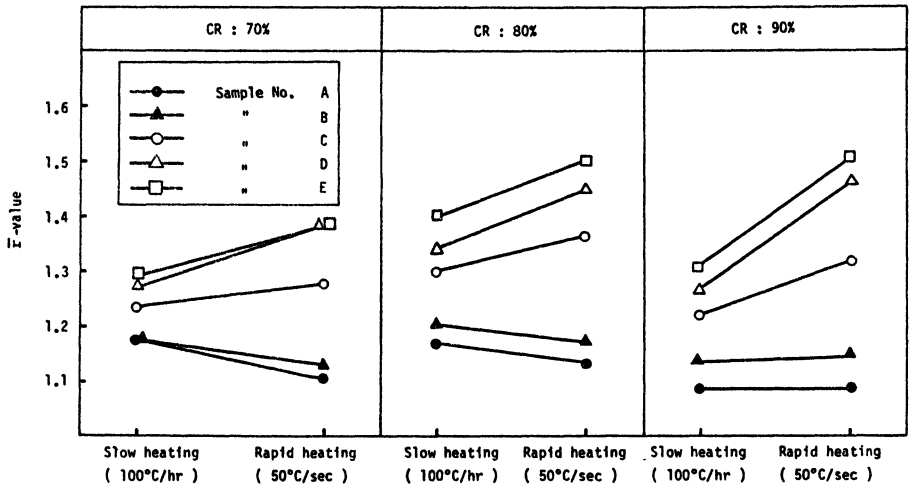

Figure 5. Effect of heating rate in annealing on r̄-value.

reduction exceeding 80%. Therefore, the cold reduction at which Δr-value is zero moves to the higher cold reduction side as the heating rate is higher.

3-3 *Texture*

Figure 6 shows the integrated reflection intensities of cold-rolled materials (heat-treated materials A: small carbide prior to cold-rolling and E: large carbide prior to cold-rolling). Figures 7 and 8 show the integrated reflection intensities of heat-treated materials A, B, C, D and E after annealing.

No difference was observed in the effect of the cold reduction on the texture of cold-rolled sheet due to carbide size prior to cold rolling. As the cold reduction becomes higher, {222} intensity increases, {110}, {332}, {321} and {310} intensities decrease slightly, and {200} and {211} intensities show almost no change.

The results of the texture after annealing are as follows:

(1) {222} intensity increases as cold reduction becomes higher for any carbide size and heating rate. In the case of slow heating, it hardly changes by the carbide size prior to cold rolling at 70 and 80% cold reduction, but it increases slightly as the carbide size becomes larger at 90% cold reduction. However, in the case of rapid heating, {222} intensities of materials C, D and E (large carbide prior to cold rolling) are much higher than those of materials A and B (small carbide prior to cold rolling). Consequently, under any cold reductions, {222} intensity of heat-treated materials A and B is a little higher in slow heating than in rapid heating, while that of heat-treated materials C, D, and E is considerably higher in rapid heating. In comparison with {222} intensity of cold-rolled materials, that of annealed

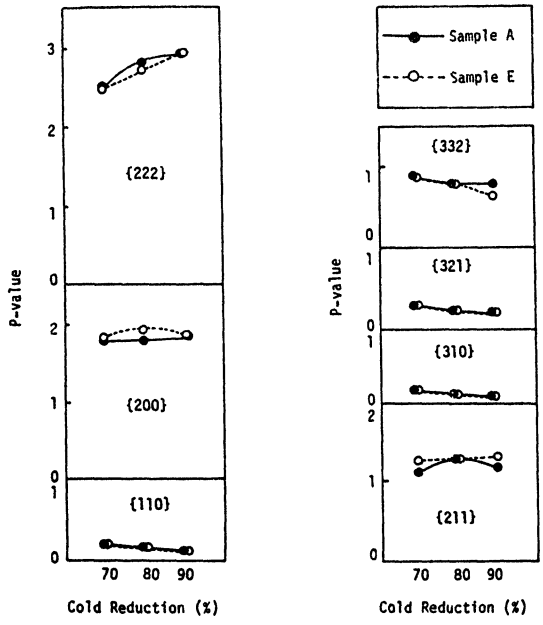

Figure 6. Effect of cold reduction on integrated X-ray reflection intensity (P-value) in cold-rolled sheet.

materials is low at 70% cold reduction, nearly equal at 80%, and high at 90% in this experiment. At 90% cold reduction, this tendency is marked when heat-treated materials C, D and E with large carbides prior to cold rolling are rapidly heated. However, this relation of {222} intensities between cold-rolled and annealed materials under the effect of cold reduction should naturally vary with chemical compositions and other conditions.

(2) The {200} intensity of annealed materials is lower than that of cold-rolled materials. Its change due to cold reduction, particularly at 90% cold reduction, shows a different tendency; that is, in the case of slow heating, it always increases remarkably at 90% cold reduction irrespective of the carbide size prior to cold rolling, and shows a tendency similar to the result reported by Whiteley.[2] In the case of rapid heating, on the other hand, the change in {200} intensity of heat-treated materials A and B with small carbide prior to cold rolling is different from that of heat-treated materials C, D and E with large carbide prior to cold rolling. There is a remarkable increase at 90% cold reduction in the former as in the case of slow heating, whereas a decrease is observed at 90% cold reduction in the latter. This is the reason for the cold reduction of the peak $\bar{r}$-value moving toward the higher cold reduction side.

(3) The {110} intensity of annealed materials is higher than that of cold-rolled materials. The effect of carbide

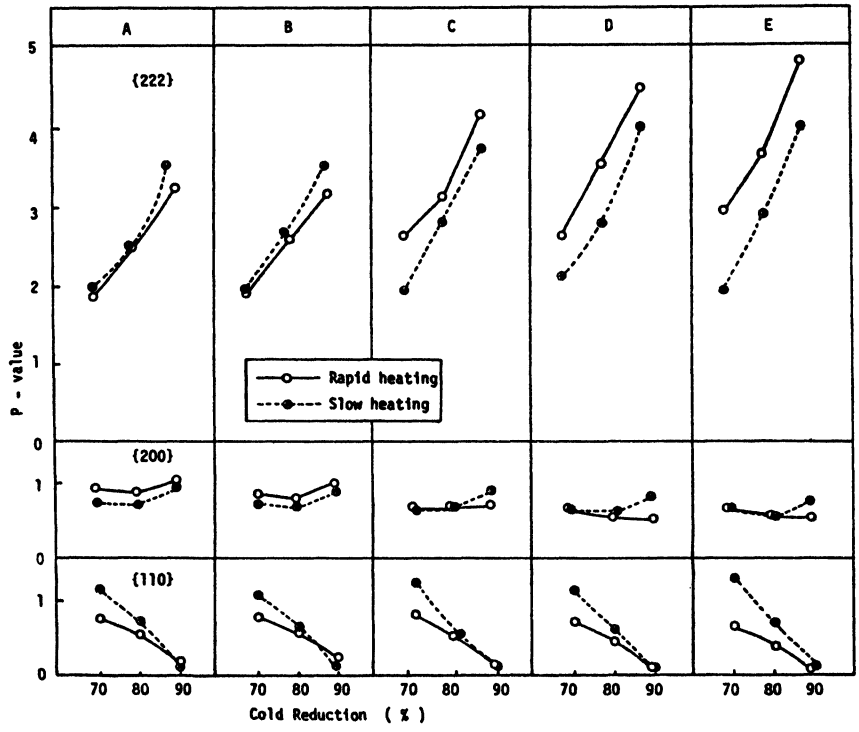

Figure 7. Effect of cold reduction on integrated X-ray reflection intensity in annealed sheet (on main three principal planes).

size on the {110} intensity is hardly recognized. The difference of its intensity with heating rate is clear at 70 and 80% cold reduction, that is, its intensity is higher in slow heating than in rapid heating.

(4) The {211} intensity of annealed materials is almost the same as that of cold-rolled materials in slow heating, but its intensity decreases as the carbide size prior to cold rolling becomes larger in rapid heating. This tendency is remarkable at 90% cold reduction.

(5) The change in {321} and {310} intensity is similar to that of {110} intensity.

(6) The {332} intensity of annealed materials is almost equal to that of cold-rolled materials. The effect of carbide size prior to cold rolling on its intensity is hardly observed.

Figures 9 and 10 respectively show the {200} pole figures of heat-treated materials A and E. As for heat-treated material A with small carbides prior to cold rolling, the main texture components are {111}<112> and {111}<110>, of which the density is higher in slow heating than in rapid heating at any

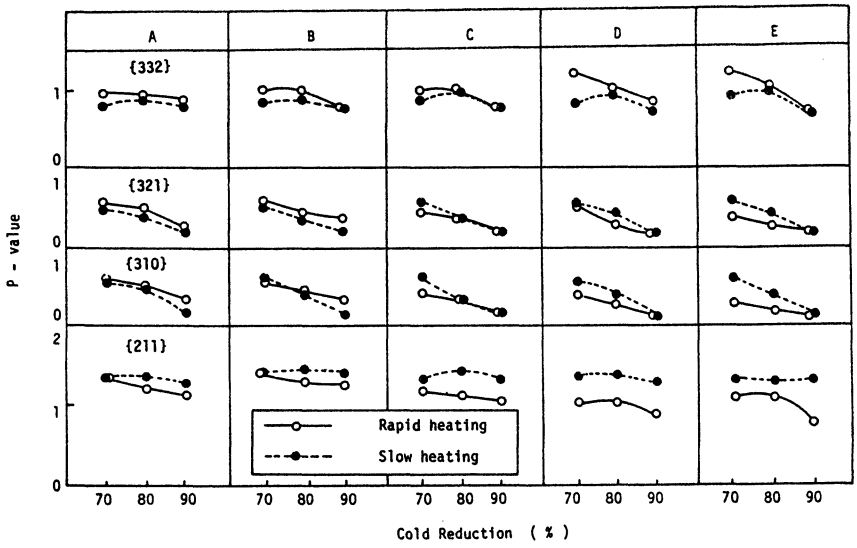

Figure 8. Effect of cold reduction on integrated X-ray reflection intensity (P-value) in annealed sheet (on the other four planes).

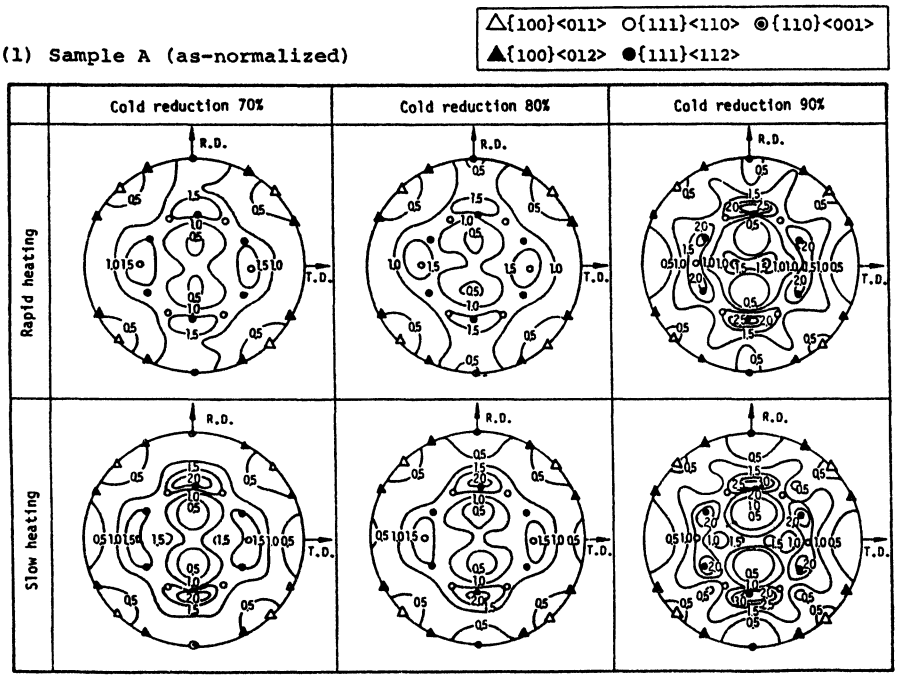

Figure 9. Effect of annealing condition and carbide size on {200} pole figure.

(2) Sample E (Normalization +800°C x 3hr)

△{100}<011> ○{111}<110> ◉{110}<001>
▲{100}<012> ●{111}<112>

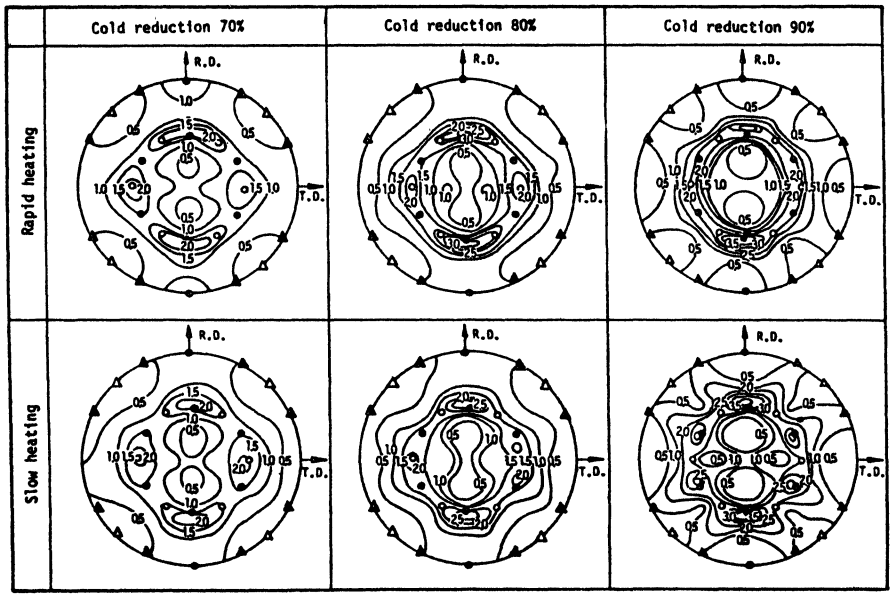

Figure 10. Effect of annealing condition and carbide size on {200} pole figure.

cold reductions. The {110}<001> density decreases as the cold reduction becomes higher both in rapid heating and in slow heating. The {111}<112> density increases markedly at 90% cold reduction, and the texture component, rotated by ±15° about the <110> direction parallel to the rolling plane increases. In the case of heat-treated material E with large carbides, {111}<112> and {111}<110> densities are higher in rapid heating than in slow heating at any cold reduction. This result is contrary to that of heat-treated material A. With an increase in cold reduction, {111}<112> and {111}<110> densities become higher in rapid heating and the {111}<112> density in slow heating. At 90% cold reduction, the texture component, rotated by ±15° about the <110> direction parallel to the rolling plane decreases in contrast with the result of heat-treated material A.

The relationship between r-value and texture has already been clarified experimentally and theoretically by many investigators,[12-15] from which it has been recognized generally that the near {111} orientations, such as {111}, {211} and {332} improve r-value and the orientations close to {100} such as {100} and {310} reduce r-value. Consequently, it is possible to explain to some extent the change in the cold reduction of the peak $\bar{r}$-value.

As for Δr-value, it is obvious that it depends on the texture, and according to the calculation made using a single crystal model, it has been clarified that {111} single crystal

has less planar anisotropy, {110}<001> single crystal shows the anisotropy of $r_{90} > r_0 > r_{45}$, and that {100}<011> and {211}<011> show the anisotropy of $r_{45} < r_{90} \approx r_0$.[14,16]

Figure 11 shows the relation between Δr-value and P{110}/(P{100} + P{211}), from which it can be seen that the larger the value of P{110}/(P{100} + P{211}), the higher is the Δr-value.

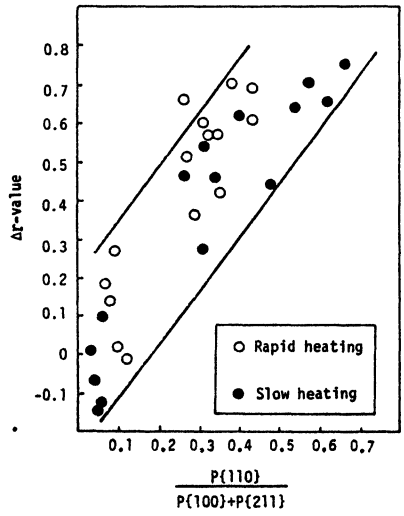

Figure 11. Relation between Δr-value and P{110}/(P{100} + P{211}).

4. CONSIDERATIONS

4-1 *Dependence of* $\bar{r}$*-value upon heating rate in annealing*

As to the effect of heating rate in annealing on r-value of cold-rolled steel sheets, there exists an optimum heating rate[17,18] for Al-killed steels depending on their Al and N contents because a high $\bar{r}$-value is developed due to the timing of cluster precipitation and recrystallization, but for the ordinary rimmed steels, $\bar{r}$-value generally tends to drop with faster heating because the preferential oriented nucleation is less remarkable at recrystallization. However, the $\bar{r}$-value with heating rate in annealing is greatly influenced by the carbide size prior to cold rolling. In the case of large carbides prior to cold rolling, it is noted that $\bar{r}$-value develops with increasing heating rate. This phenomenon can be observed not only in rimmed steels, but also in Al-killed steels which are high-temperature coiled at hot rolling.[19] The dependence of $\bar{r}$-value on heating rate in annealing under the effect of carbide sizes prior to cold rolling are shown schematically in Figure 12, from which it is noted that

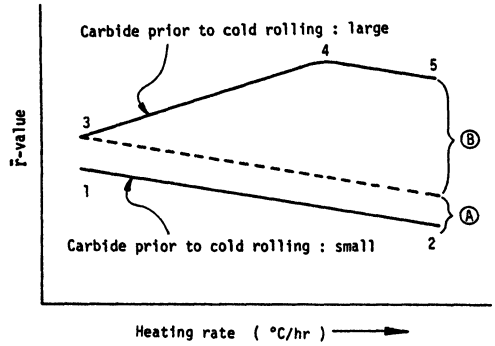

Figure 12. Schematic representation of the effect of heating rate in annealing on $\bar{r}$-value.

(1) When the carbide size prior to cold rolling is small, the faster the heating rate in annealing, the lower the $\bar{r}$-value.

(2) When the carbide size prior to cold rolling is large, the faster the heating in annealing, the higher is the $\bar{r}$-value, and when the heating is made extremely fast, the $\bar{r}$-value tends to decrease.

(3) When the carbide size prior to cold rolling is larger, the $\bar{r}$-value is higher in slow heating than that of small carbides, and as the heating becomes faster, the difference in $\bar{r}$-value with carbide size prior to cold rolling becomes larger as described in (1) and (2) above.

When the reasons for difference in the dependency of $\bar{r}$-value on the heating rate in annealing with the carbide size prior to cold rolling are considered in Figure 12, it may be suspected as follows ($\bar{r}$-values at the locations, 1, 2, 3, 4, and 5 shown in the figure are expressed by $\bar{r}_1$, $\bar{r}_2$, $\bar{r}_3$, $\bar{r}_4$, and $\bar{r}_5$):

(i) Reasons for $\bar{r}_3 > \bar{r}_1$ Ⓐ

This is considered to depend on the effect of the carbide size. Deformation microstructure of matrix adjacent to carbide at cold rolling differs from that of ferrite far apart from carbide (cannot be distinguished from the changes in texture), and the nucleation of {111} orientation is hindered in the ferrite region around the carbide. Consequently, with the same carbon content, the larger the carbide, the less is the ferrite region around the carbide, and the higher is the $\bar{r}$-value. This has little to do with the heating rate.

(ii) Reasons for $\bar{r}_1 > \bar{r}_2$

This is considered to depend on the effect of nucleation and recrystallization temperature. As the heating rate is faster, unfavorable nuclei to $\bar{r}$-value are formed, and solute

carbon increases with the rise in recrystallization temperatures (the lesser solute carbon, the higher is $\bar{r}$-value, and the effect of solute carbon will be discussed later).

(iii) Reasons for $\bar{r}_4 > \bar{r}_3$ Ⓑ

This is supposed to depend on the interaction of solute carbon and recrystallization temperatures: favorable effect of having lesser solute carbon during recrystallization and unfavorable effect with faster heating described in (ii) above. The former effect is far greater than the latter. When the carbide size prior to cold rolling is large, the faster the heating, the slower is the dissolution of carbides, and the lesser is the solute carbon. The effect of carbon content on the $\bar{r}$-value according to authors under the condition of small carbides is shown in Figure 13.[20] From this

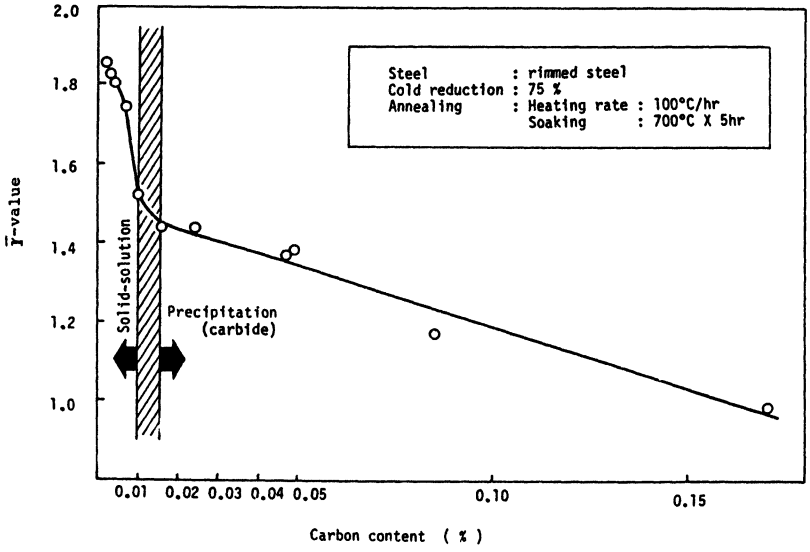

Figure 13. Effect of carbon content on $\bar{r}$-value.

figure, it is noted that $\bar{r}$-value becomes higher with the decrease in the carbon content, but the increase in $\bar{r}$-value varies remarkably at about 0.01% carbon, and $\bar{r}$-value becomes much higher at less 0.01% carbon. The change in $\bar{r}$-value in the high-carbon regions is due to the amount of carbides, and the change in $\bar{r}$-value in the low-carbon regions under the effect of the amount of solute carbon. In view of these facts, it is clear that the effect of carbon on the $\bar{r}$-value is far greater with carbon existing in the form of solute than with carbon existing in the precipitated condition.

(iv) Reasons for $\bar{r}_4 > \bar{r}_5$

When the heating rate becomes extremely fast, the delay in dissolution of carbides reaches the limit, and there remains only an unfavorable effect caused by faster heating described in (ii).

From these reasons given above, the difference in the $\bar{r}$-values caused by the carbide size prior to cold rolling consists of Ⓐ + Ⓑ, of which Ⓑ represents the increase in $\bar{r}$-value caused by the heating rate.

Next, the change in texture caused by the heating rate is considered. Although almost no change was observed in cold-rolled texture with the carbide size, the deformation microstructure during cold rolling in the matrix around the carbides differs from that in the matrix far apart from the carbides, and this difference is supposed to be one of the causes exerting influence on the recrystallization texture. The recrystallization texture seems to be influenced greatly by {111} nucleation at the initial stage of recrystallization. The change of {222} intensity from cold-rolled state to recovery state is hardly observed, but it tends to decrease once from the initial to the middle stages of recrystallization (nucleation period) and increase again at the middle and final stages (nucleus growth period).

This change in {222} intensity is supposed to be caused by the amount of interstitials (C, N), the amount and distribution of carbides, and carbide size prior to cold rolling. In the case of large carbide prior to cold rolling, the {222} intensity does not greatly decrease at the initial stage and increases greatly at the middle and final stage of recrystallization. This tendency is clearly observed particularly in rapid heating. The {222} intensity hardly decreases with the decrease in manganese content at the initial stage of recrystallization.[21,22]

In addition, there are some other investigators reporting that the increase in $\bar{r}$-value in rapid heating is due to MnS cluster.[23] However, the authors do not recognize this phenomenon in the case of carbide-free materials prior to cold rolling.[19] Consequently, the effect of MnS cluster is supposed to be less than that of the carbide size on the increase in $\bar{r}$-value in rapid heating.

4-2 *Cold reduction of peak $\bar{r}$-value*

The cold reduction at which $\bar{r}$-value reaches maximum is very important for the manufacture of cold-rolled steel sheets, and the authors have been studying the cold reduction of peak $\bar{r}$-value. The factors that have been known so far are as follows:

(1) The less the carbon content, the higher is the cold reduction of peak $\bar{r}$-value.

(2) A higher annealing temperature leads to a higher cold reduction of peak $\bar{r}$-value.

(3) A better lubrication at cold rolling results in a higher cold reduction of peak $\bar{r}$-value.

In the present experiments, an interesting phenomenon different from these factors has been recognized; that is, the cold reduction of peak $\bar{r}$-value in slow heating (box-annealing) is near 80%, but in rapid heating (continuous annealing), the cold reduction of peak $\bar{r}$-value varies with the carbide size prior to cold reduction. In rapid heating the cold reduction of peak $\bar{r}$-value moves to the higher cold reduction side as the carbide size prior to cold rolling becomes larger, and $\bar{r}$-value becomes higher at a cold reduction of 90% than 80%.

The reason for the cold reduction of peak $\bar{r}$-value moving to the higher cold reduction side may be explained by such factors as cold reduction, recrystallization temperature varying with heating rate and the resultant change in solute carbon at the initial stage of recrystallization and nucleation. The recrystallization temperature becomes lower with the increase in cold reduction. In the present experiments, the recrystallization temperature at 90% cold reduction is lower by about 30° to 40°C than that at 80% cold reduction. Also, the recrystallization temperature in rapid heating is higher by 100° to 120°C than that in slow heating. Furthermore, in rapid heating, the effect of the recrystallization temperature on the cold reduction of peak $\bar{r}$-value is greater because of the delay in dissolution of carbide. In slow heating, on the other hand, there is almost no effect of the difference in solute carbon caused by recrystallization temperature because the carbide dissolves up to the equilibrium and the recrystallization temperature becomes low.

These tendencies are shown in Figure 14, an Fe-C equilibrium phase diagram, where t_1 (90% cold reduction) and t_2 (80% cold reduction) are the recrystallization temperatures

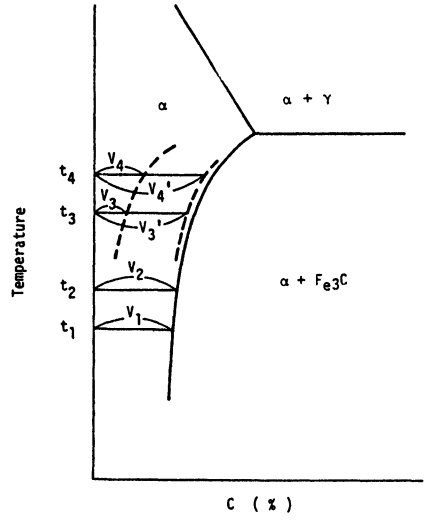

Figure 14. Schematic representation of recrystallization temperature and solute carbon content in Fe-C phase diagram.

in slow heating, t_3 (90% cold reduction) and t_4 (80% cold reduction) are the recrystallization temperatures in rapid heating, and V_1, V_2, $V_3(V_3')$ and $V_4(V_4')$ are the amount of solute carbon at the recrystallization temperatures.

When the carbide size prior to cold reduction is large, the amount of solute carbon at the recrystallization temperature in rapid heating is slight (V_3, V_4), and it decreases from V_4 to V_3 as the cold reduction becomes higher from 80 to 90% because of the lowering of the recrystallization temperature. This promotes {111} preferred nucleation and improves $\bar{r}$-value.

In slow heating, the amount of solute carbon (V_2) at 80% cold reduction is nearly equal to that of solute carbon (V_1) at 90% cold reduction, because of the low recrystallization temperature and dissolution of carbides up to the equilibrium. As a result, the improvement of the $\bar{r}$-value with an increase in cold reduction as shown in rapid heating is hardly observed.

On the other hand, the small-size carbide prior to cold rolling dissolves easily up to the near equilibrium (V_3', V_4'); therefore the difference in the $\bar{r}$-value under the effect of cold reduction is less than in the case of large carbides prior to cold rolling.

In view of these considerations, it can be considered that when the carbide size prior to cold rolling is large, {111} preferred nucleation is promoted in rapid heating, and the cold reduction of peak $\bar{r}$-value moves from 80% cold reduction (in the case of small carbides) to 90%.

4-3 *Correspondence to hot coiling temperature*

In the present experiments, the carbide size prior to cold rolling has been changed by the heat treatment at the laboratory, but in manufacturing it is controlled by the hot coiling temperature.

With a view to investigating the correspondence of our heat treatments in the laboratory to hot coiling conditions in manufacturing, the following experiments were conducted with the three low carbon capped hot bands coiled at different temperatures; 600°C (small carbide), 650°C (medium carbide), and 680°C (large carbide). These coiling temperatures represent the temperature at the surface of the bands measured by a radiation thermometer, and the true temperature at the interior is higher by 80°-90°C.

These hot bands were cold rolled; the cold reduction ranged from 50 to 90%, and annealed in rapid heating. The results of $\bar{r}$ and Δr-values are shown in Figure 15. These results are in excellent agreement with those obtained from our heat treatment in the laboratory. The changes in carbide size by our heat treatment in the laboratory correspond well with those obtained by controlling hot coiling conditions in manufacturing.

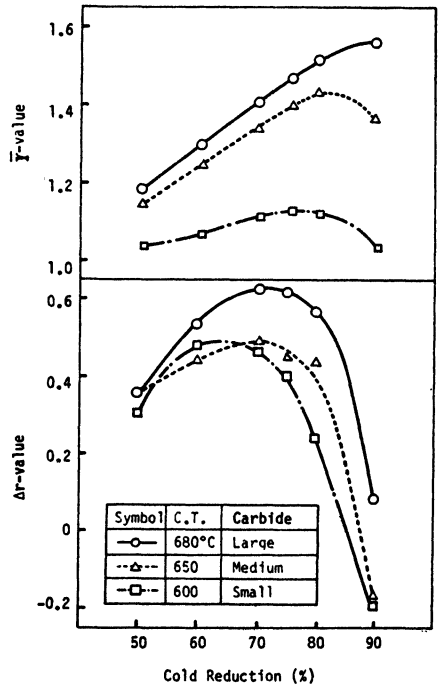

Figure 15. Effect of cold reduction on $\bar{r}$-value at different hot coiling temperature.

5. CONCLUSIONS

The following results have been obtained from the investigations on the effects of the carbide size prior to cold rolling, cold reduction, and heating rate in annealing on the deep-drawability of low-carbon, capped cold-rolled steel sheets:

(1) The influence of heating rate in annealing on $\bar{r}$-value largely depends upon the carbide size prior to cold rolling. That is, when the carbide size prior to cold rolling is large, $\bar{r}$-value becomes higher in slow annealing as in box annealing as compared with the case where the carbide size prior to cold rolling is small. Moreover, when the carbide size prior to cold rolling is small, $\bar{r}$-value lowers with increasing heating rate in annealing, but when large, $\bar{r}$-value becomes higher with heating rate, and higher $\bar{r}$-value is obtained in rapid heating as in continuous annealing.

(2) The cold reduction of peak $\bar{r}$-value depends on the carbide size prior to cold rolling and heating rate in annealing. In slow heating, the cold reduction of peak $\bar{r}$-value is nearly constant irrespective of the carbide size prior to cold rolling, but in rapid heating, the larger the carbide size prior to cold rolling, the higher is the cold reduction of peak $\bar{r}$-value.

(3) Δr- value with large carbides prior to cold rolling is somewhat higher than that with small carbides. The cold reduction of peak Δr-value is a little higher in rapid heating than in slow heating, and hence, the cold reduction at which Δr-value becomes zero moves to the higher cold reduction side.

REFERENCES

1. W. T. Lankford, S. C. Snyder and J. A. Bauscher, *Trans. ASM.*, 42, 1197 (1950).
2. R. L. Whiteley and D. W. Wise, *Flat Rolled Products III*, 16, 47 (1962).
3. M. Fukuda, *JISI of Japan*, 53, 559 (1967).
4. S. Teshima and M. Shimizu, *Mech. Working of Steel II*, AIME, 279 (1965).
5. K. Matsudo and T. Shimomura, *Trans. ISIJ*, 10, 448 (1970).
6. P. R. V. Evans, J. C. Biteon and I. F. Hughes, *JISI*, 207, 331 (1969).
7. H. Takechi, N. Takahashi, S. Osada and S. Nagao, *JISI of Japan*, 56, 475 (1970).
8. J. F. Held, *Trans. AIME*, 239, 573 (1967).
9. K. Matsudo and Y. Uchida, *Preprint of J. Japan Inst. Metals*, 10, 143 (1969).
10. H. Naemura, Y. Fukuoka, S. Osaka and H. Ishioka, *Nippon Kokan Technical Report*, 73, 47 (1977).
11. M. H. Mueller, W. P. Chernock and P. A. Beck, *Trans. AIME*, 212, 39 (1958).
12. R. S. Burns and R. H. Heyer, *Sheet Metal Ind.*, 35, 261 (1958).
13. M. Fukuda, *T. Japan Soc. Tech. Plasticity*, 5, 3 (1964).
14. R. W. Vieth and R. L. Whiteley, *3rd International Colloquium of IDDRG*, London (1964).
15. S. Nagashima, H. Takechi and H. Kato, *J. Japan Inst. Metals*, 29, 393 (1965).
16. T. Okamoto, T. Shiraiwa and M. Fukuda, *Sumitomo Metals*, 14, 123 (1962).
17. M. Shimizu, K. Matsukura, N. Takahashi and Y. Shinagawa, *JISI of Japan*, 50, 2094 (1964).
18. K. Matsudo, *J. Japan Soc. Tech. Plasticity*, 7, 376 (1966).
19. K. Matsudo, T. Shimomura, H. Kobayashi and O. Nozoe, *JISI of Japan*, 61, 424 (1975).
20. K. Matsudo, T. Shimomura and H. Kobayashi, *Preprint of Symposium of J. Japan Inst. Metals*, 10, 105 (1971).
21. H. Hu and S. R. Goodman, *Met. Trans.*, 1, 3057 (1970).
22. I. F. Hughes and E. W. Page, *Met. Trans.*, 2, 2067 (1971).
23. K. Toda, H. Gondoh, H. Takechi, et al., *JISI of Japan*, 61, 2363 (1975).